Effect Of Variable Particle Sizes On Carbon Steel In Oil/Water Slurries

***Ghaith Abdulrahman & ** Khulud Rahuma**

Abstract

This work aims to study the effect of particle sizes on carbon steel in oil/20% water environments containing particle sized 600-710μm and 150-300 μm (Al_2O_3) have been investigated by erosion test rig. The results were used to constructed erosion–corrosion mechanism, synergism and wastage maps, as a function of impact angle and velocity. In addition, the results indicate that the corrosion rate (kc) was increased with an increase in potentials from negative potential to positive applied potential. There was little enhancement of increased erosion contribution (ke) with an increase in potentials due to corrosion enhanced erosion. On the other hand, the total volume loss erosion-corrosion (kec) was increased with an increase in the impact velocities and particle size from 150-300μm to 600-710 μm in oil/20% water test environment. However, the value of corrosion contribution was increased with decrease in particle size from 600-710μm to150-300 μm. In addition, the volume loss of erosion contribution (ke) was high in the oil/water environment containing particle sized 600-710μm compared with particle sized 150-300μm.

Key words; Steel, Oil, Water, Particles, Size

*Staff member, Petroleum Eng. Dept. University of Ajdabiya, Libya

**Staff member, Petroleum Eng. Dept. University of Tripoli, Libya

1-Introduction

Erosion–corrosion in oil production depends on a range of factors present in downhole oil wells, such as sand concentration, reservoir pressure, temperature, and H2S and CO2 concentration, which cause mechanical damage to the electrical submersible pump, leading to economic losses due to maintenance, leaks and exchanging of parts[1-2]. Sand production from reservoirs with oil can be controlled by designing a Gravel Pack that prevents sand from being produced with the oil from upstream to downstream [5]. The effect of sand on material is dependant on the shape of the sand particles; sharp particles caused more damage than round particles. Erosion by solid particle impacts on a brittle substrate is caused by the formation and intersection of cracking. The types of crack that form on the erodent surface are dependent on the erosive particle shape and size. Lawn and Wilshaw [6], and Swan and Hagan [7] have reported that the impact of large round particles, greater than 200 μm in size, causes cracking, while small particles cause plastic deformation of the surface of the specimen. The effect of particle size on the erosion rate of materials generally increases with an increase in erodent particle size. The effect of particle hardness becomes clearer when the high hard particle impacts on the surface of the specimen, such as erosion of mild steel by alumina particles [8]. In this paper, the effects of impact angle and velocity were assessed for carbon steel in a range of crude oil/ water slurries. Erosion-corrosion maps were generated based on the results showing the variation in wastage and regime of degradation as a function of these variables.

2. Experimental details

Erosion-corrosion test methods

The erosion–corrosion tests were carried out using an impinging jet apparatus is described elsewhere [9]. This consisted of a jet of particles in an aqueous flow enabling the effect of erosion variables to be evaluated independently of each other. The impact angle of the specimen could be varied by rotating the stationary specimen. The velocity was calibrated through knowledge of the geometry of the outlet jet. The slurry was composed of aluminum oxide (Al_2O_3) 150-300 μm and 600-710μm, as shown in Figs.1 (a) and (b), in solution of Na_2CO_3 + $NaHCO_3$ and crude oil pH value was 8.25 at room temperature.

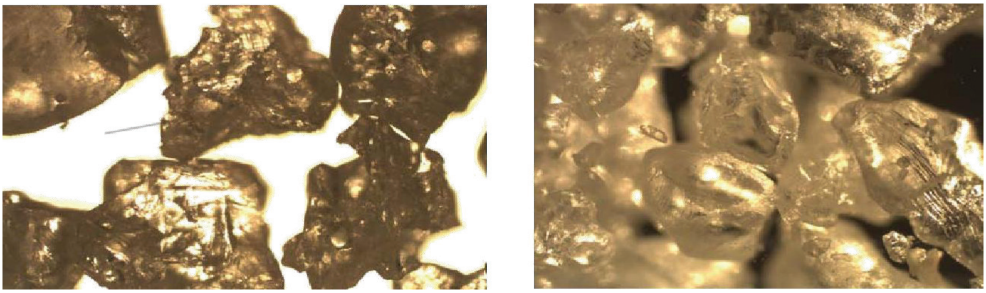

(a) **Aluminum oxide(Al_2O_3)** (b) **Reservoir water**

Fig. 1: Optical microscopy of aluminum oxide used in the erosion-corrosion test rig :(a) 600-710μm (b) 150-300μm.

The test specimen was connected to an electrochemical cell as shown in Figs.2. The reference electrode was Saturated Calomel. Potentiodynamic polarization curves were measured through sweeping the potential in a positive direction from –800 to 800 mV at a sweep rate of 200 mV min^{-1} during the test.

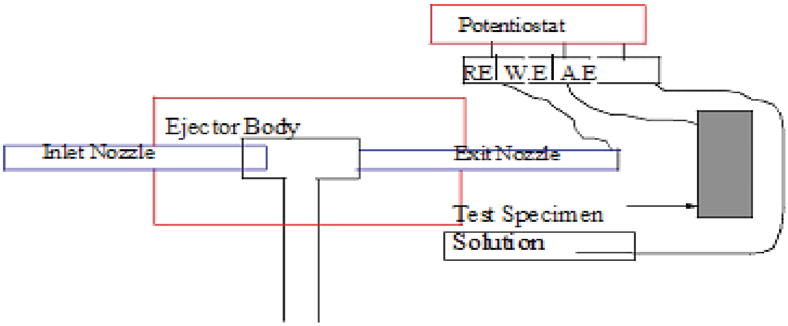

Fig. 2: Electrochemical connection in the slurry erosion test.

Erosion–corrosion tests were conducted at three applied potentials namely, -400 mV, 0 mV and 400mV (SCE) for 30 minutes using a computer controlled ACM potentiostatic. The test material was carbon steel supplied by Kelvin Steel Glasgow with chemical composition as percentage: C: 0.18, Mn 1.6, Si 0.55, Cr 0.25, Cu: 0.35, Ni: 0.3, S: 0.008. The chemical composition of crude oil in ppm (mass) was (Ca: 33.26, Na: 4.26, K: 1.07, H2S: 0.0007). The specific gravity was 0.7674 and density was 767 g l^{-1}. The dimensions of the specimens were 25mm × 10mm × 4 mm. The area exposed to impingement jet was 0.19cm^2, whilst the remaining area was covered by a coating in order to ensure that all corrosion measurements related to the erosion-corrosion process only. Mass change measurements were made of the samples post testing using a Metter electronic balance. The tests were carried out at three impact velocities i.e. 2.5, 3.5 and 4.5 m s^{-1}**,** for 30 minutes. The reproducibility of the experiments was estimated to be ± 5% calculated between two-three consecutive experiments. At the end of the test, the samples were cleaned with distilled water to remove any deposited material. Following exposure, the morphology of the eroded.

3. Results

Polarization curves

The polarization curves of the samples were investigated using a computer AC Gill potentiostat in crude oil/20%water. The corrosion testing was conducted under Potentiodynamic conditions, where samples were polarized at potentials 15°, 45° and 90°, to observe the effect of corrosion attacks on material. Figures 3-5(a-b) show the polarization curves for the carbon steel in crude oil / 20% water environments at various impact velocities and impact angles. There was a clear difference between the effects of impact angles on the carbon steel. The polarization curve tended to shift to higher current densities with higher velocities. However, it was found that with the large particle size 600-710 μm there was a lower current density than at small particle size 150-300 μm.

Polarization curves in Fig.3(a) show that following erosion-corrosion in the oil/water environment containing particle size 600-710 μm at impact angle of 15°, there was a general increase in current density with increasing velocity from 2.5 to 4.5 ms^{-1}. Clear evidence of passivation was observed at low velocity 2.5ms^{-1}. Fig. 3(b) shows that following erosion-corrosion in the oil/water environment containing particle size 150-300 μm at impact angle of 15°, there was a general increase in current density with decreasing in particle size. A similar pattern was observed for the carbon steel in the oil/water environments at impact angles 45° and 90°, shown in Fig. 4-5(a-b), with current density increasing with impact angle.

In addition, the value of current density of carbon steel in oil/water containing small particle was greater than the value of corrosion with large particle 600-710 μm .In general the value of current was increased with increasing in velocity for carbon steel with particle sizes 600-710 μm and 150-300 μm. Because, an increase in the velocity indicates removal of the passive film and the value of corrosion is increased [2].

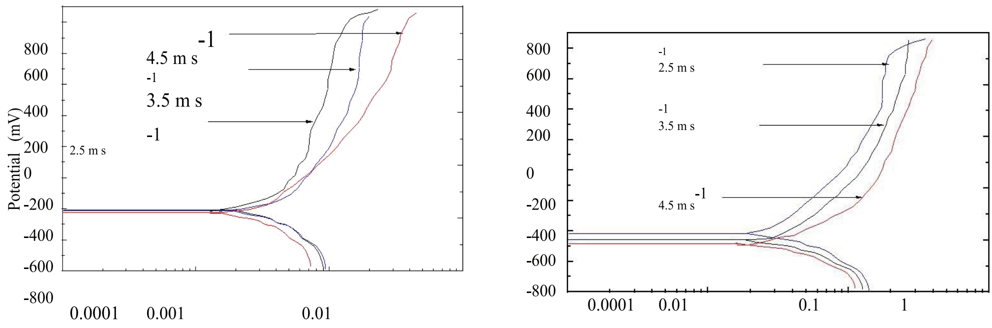

(a) Current (mA cm^{-2}) (b) Current (mA cm^{-2})

Fig. 3: Polarization curves for carbon steel at various impact velocities in oil /20% water, at impact angle 15° and particle size (a) 600 –710μm (b) 150-300μm

μm

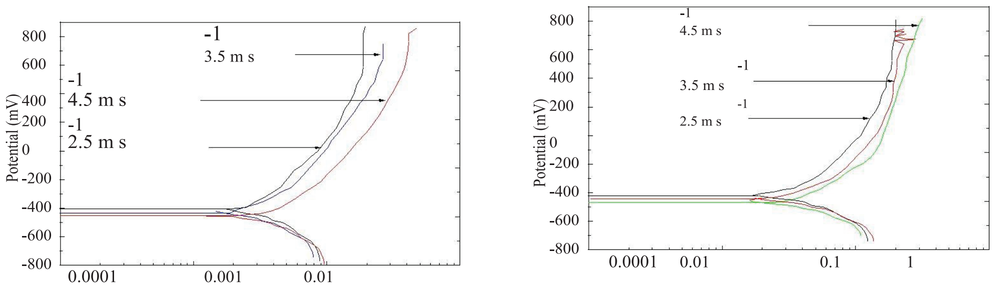

(a) Current (mA cm^{-2}) (b) Current (mA cm^{-2})

Fig. 4: Polarization curves for carbon steel at various impact velocities in oil /20% water, at impact angle 45° and particle size (a) 600 –710μm (b) 150-300μm

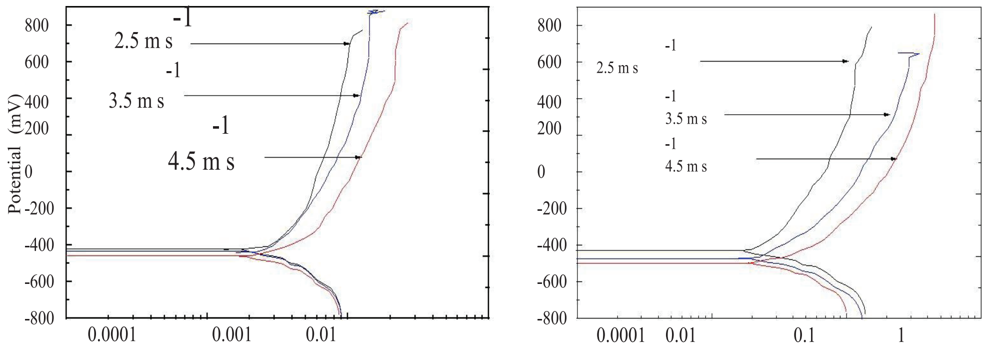

(a) Current (mA cm^{-2}) (b) Current (mA cm^{-2})

Fig. 5: Polarization curves for carbon steel at various impact velocities in oil /20% water, at impact angle 90° and particle size (a) 600 –710μm (b) 150-300μm

Volume loss

The mass loss has been constructed as a function of impact velocity, impact angles and potentials. The erosion contribution ke can be expressed from the calculation of the corrosion contribution kc and the total erosion corrosion contribution kec [1-4]:

$$Kec = ke + kc \qquad (1)$$

Kec is the interaction between the mechanical and electrochemical damage processes, erosion and corrosion can enhance each other.

$$Ke = keo + \Delta ke \qquad (2)$$

$$Kc = kco + \Delta kc \qquad (3)$$

Where keo is the pure erosion, kco is the pure corrosion, Δkc is the corrosion-enhanced erosion (corrosion due to erosion), and ke is the erosion-enhanced corrosion (erosion due to corrosion). Tables 1-6 show the results of the calculations of volume loss for ke, kc and kec for carbon steel in oil/20% water at difference particle sizes, impact velocities with various impact angles at various applied potentials.

Fig.6 (a-c) shows mass loss as a function of impact velocity and impact angles for carbon steel in the crude oil /20% water environment containing particle size 600-710μm at potential of - 400mV. Generally, there was an increase in the erosion corrosion contribution (Kec) with increasing in impact velocity and that consistent with the above polarization curves results and pervious investigators [1-3]. On the other hand, the erosion contribution was increased with an increase in impact velocity and impact angle. It is interesting that the corrosion rate (kc) was slowly increased with an increase in impact velocity compared with erosion contribution (ke) (Figures 6. a-c).

Fig. 7 (a-c)shows the total volume loss rate (kec) for carbon steel in oil/water environment containing particle size 600-710μm increased with an increase potential, and the total volume loss reached a peak at an impact velocity of 4.5 m s^{-1} and an impact angle of 45^{o} about 8.94mg cm $^{-2}$ h^{-1}. Moreover, the total mass loss gradually increased with a reduction in the impact angle from 90^{o} to 15^{o} and an increase in impact velocities at applied potential 0mV.In addition, the percentage of corrosion contribution was greater than the percentage of corrosion contribution compared with at negative potential -400mV, which could be due to an increase in the current density at this applied potential (0 mV).

Fig.8(a-c) shows that volume loss due to corrosion contribution (kc) for carbon steel in oil/water environment containing particle size 600-710μm. reached a peak value with an applied potential of 400 mV, which means and confirm that the current density was increased with an increase in potential, then there was an increase in the corrosion contribution [1- 3].

Figure.9-11 (a-c) shows volume loss as a function of impact velocity and impact angles for carbon steel in the 20% water with crude oil environment containing particle size 150-300μm at applied potentials of -400 mV, 0mV and 400mV. It can be noted that the values of corrosion contribution Kc increased compared with erosion contribution ke in the environment containing particle size 60-710μm , and the peak value was about 4.55 mg cm $^{-2}$ h^{-1} at impact angle 45° and velocity 4.5 m s^{-1}.

The peak value of erosion contribution (ke) in the combined environments was about 2.53 mg cm $^{-2}$ h^{-1} at 45° and velocity 4.5 m s^{-1} at cathodic potential(-400mV). However, the values of erosion contribution were smaller than the values of corrosion contribution, as shown in tables 1-6 might due to passive film on the surface of specimen.

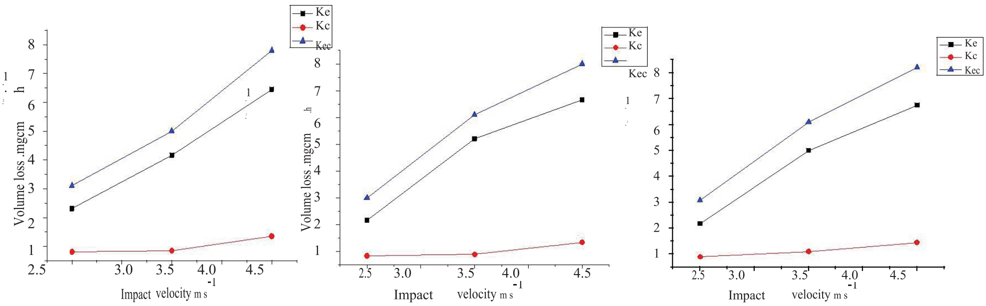

(a) (b) (c)

Fig. 6: Volume loss as function of impact velocity for carbon steel in oil /20% water at constant -400 mV and particle size 600 –710μm (a) 15° (b) 45° (c) 90°.

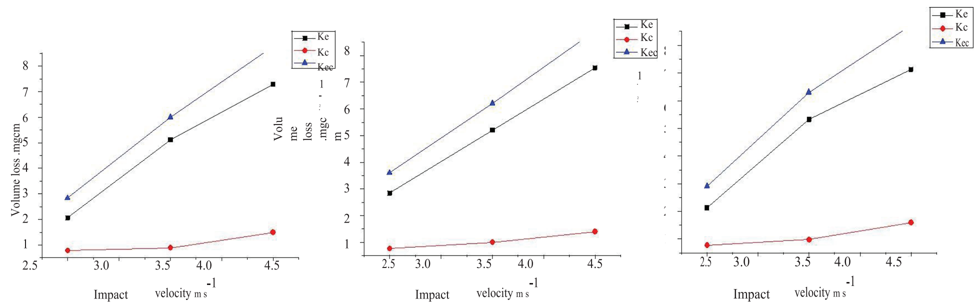

(a) (b) (c)

Fig.7: Volume loss as function of impact velocity for carbon steel in oil /20% water at 0 mV and particle size 600 –710μm (a) 15° (b) 45° (c) 90°.

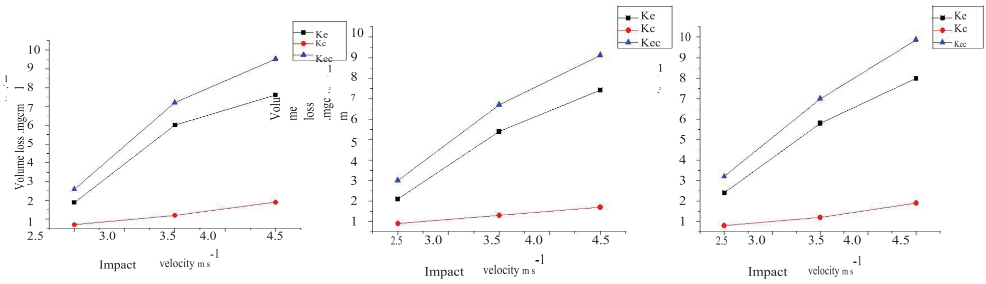

(a) (b) (c)

Fig.8: Volume loss as function of impact velocity for carbon steel in oil /20% water at 400 mV and particle size 600 –710μm (a) 15° (b) 45° (c) 90°.

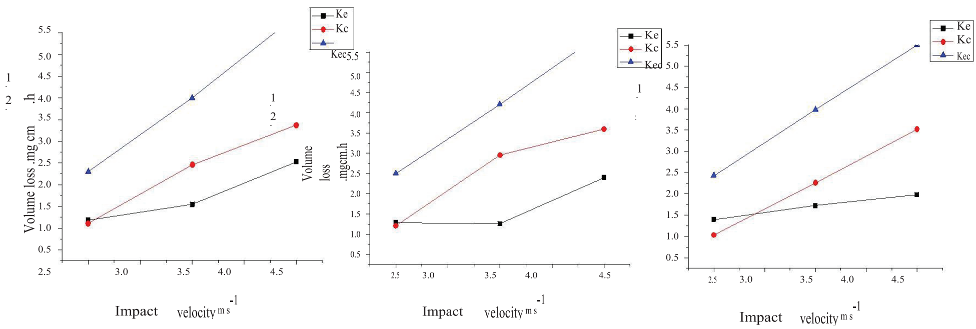

(a) (b) (c)

Fig. 9: Volume loss as function of impact velocity for carbon steel in oil /20% water at constant -400 mV and particle size 150 –300μm (a) 15° (b) 45° (c) 90°.

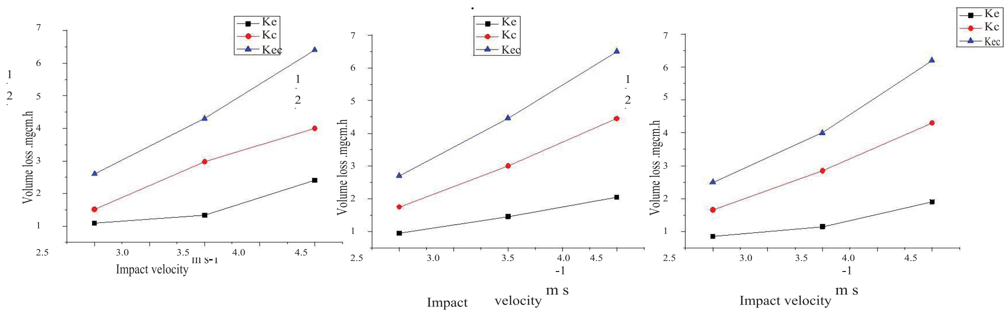

(a) (b) (c)

Fig. 10: Volume loss as function of impact velocity for carbon steel in oil /20% water at constant 0 mV andparticle size 150 –300μm (a) 15° (b) 45° (c) 90°.

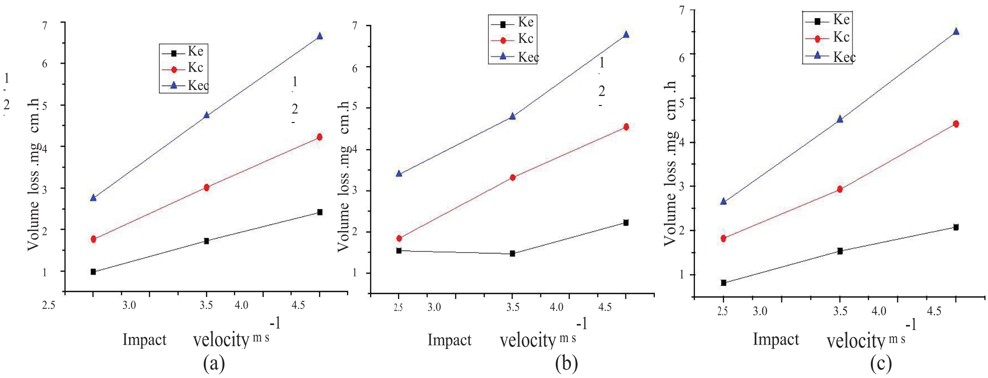

Fig. 11: Volume loss as function of impact velocity for carbon steel in oil /20% water at constant 400 mV and particle size 150 –300μm (a) 15° (b) 45° (c) 90°.

Tables.1: Volume loss as function of velocities for carbon steel in oil /20% water at - 400mV and particle size 600 –710μm (a) 15° (b) 45°(c) 90°

(a)

Velocities $m\ s^{-1}$	Ke	Kc	Kec	Ke/Kc	Δke/Δkc
2.5	2.31	0.8	3.11	2.9	-2.75
3.5	4.16	0.84	5	4.95	-26.5
4.5	6.45	1.35	7.8	4.7	-57

(b)

Velocities $m\ s^{-1}$	Ke	Kc	Kec	Ke/Kc(mg	Δke/Δkc
2.5	2.16	0.84	3	2.5	1.18
3.5	5.2	0.9	6.1	5.7	18.6
4.5	6.66	1.34	8	4.97	24.71

(c)

Velocities $m\ s^{-1}$	Ke	Kc	Kec	Ke/Kc(mg	Δke/Δkc
2.5	2.18	0.9	3.08	2.42	2.08
3.5	5	1.1	6.1	4.54	9.21
4.5	6.75	1.45	8.2	4.65	14.2

Tables.2: Volume loss as function of velocities for carbon steel in oil /20% water , at 0mV and particle size 600 –710μm (a) 15° (b) 45° (c) 90°

(a)

Velocities m s^{-1}	Ke	Kc	Kec	Ke/Kc	Δke/Δkc
2.5	2.06	0.78	2.84	2.64	-1
3.5	5.11	0.89	6	5.74	-93.6
4.5	7.28	1.5	8.78	4.85	18.4

(b)

Velocities m s^{-1}	Ke	Kc	Kec	Ke/Kc	Δke/Δkc
2.5	2.84	0.76	3.6	3.73	-23.5
3.5	5.2	1	6.2	5.2	28
4.5	7.54	1.4	8.94	5.38	21.7

(c)

Velocities m s – 1	Ke	Kc	Kec	Ke/Kc	Δke/Δkc
2.5	2.13	0.78	2.91	2.73	-21.5
3.5	5.32	0.98	6.3	5.42	16.35
4.5	7.12	1.6	8.72	4.45	13.0

Tables.3: Volume loss as function of velocities for carbon steel in oil /20% water , at 400mV and particle size 600 –710μm (a) 15° (b) 45° (c) 90°

(a)

Velocities m s^{-1}	Ke	Kc	Kec	Ke/Kc	Δke/Δkc
2.5	1.89	0.71	2.6	2.66	1
3.5	6.01	1.2	7.21	5.0	18.55
4.5	7.61	1.9	9.51	4.0	-40.1

(b)

Velocities m s^{-1}	Ke	Kc	Kec	Ke/Kc	Δke/Δkc
2.5	2.1	0.9	3	2.3	1.3
3.5	5.4	1.3	6.7	4.15	6.5
4.5	7.42	1.7	9.12	4.36	-52.75

(c)

Velocities m s^{-1}	Ke	Kc	Kec	Ke/Kc	Δke/Δkc
2.5	2.4	0.8	3.2	3	35
3.5	5.8	1.2	7	4.83	10.41
4.5	7.98	1.89	9.87	4.22	-43.4

Tables.4: Volume loss as function of velocities for carbon steel in oil /20% water, at -400mV and particle size 150 –300μm , (a) 15° (b) 45° (c) 90°.

(a)

Velocities m s^{-1}	Ke	Kc	Kec	Ke/Kc	Δke/Δkc
2.5	1.1	1.11E+00	2.3	1.07	3.5
3.5	1.5	2.46E+00	4	0.62	0.49
4.5	2.53	3.37E+00	5.9	0.75	0.573

(b)

Velocities m s^{-1}	Ke	Kc	Kec	Ke/Kc	Δke/Δkc
2.5	1.2	1.21E+00	2.5	1.06	0.91
3.5	1.26	2.95E+00	4.21	0.42	0.19
4.5	2.4	3.60E+00	6	0.66	0.29

(c)

Velocities m s^{-1}	Ke	Kc	Kec	Ke/Kc	Δke/Δkc
2.5	1.3	1.03E+00	2.43	1.35	2.76
3.5	1.72	2.26E+00	3.98	0.764	0.65
4.5	1.98	3.52E+00	5.5	0.56	0.42

Tables.5: Volume loss as function of velocities for carbon steel in oil /20% water, at 0 mV, and particle size 150 –300μm , (a) 15° (b) 45° (c) 90°.

(a)

Velocities m s^{-1}	Ke	Kc	Kec	Ke/Kc	Δke/Δkc
2.5	1.1	1.51E+00	2.6	0.72	0.9
3.5	1.33	2.97E+00	4.3	0.45	0.27
4.5	2.4	4.00E+00	6.4	0.6	0.37

(b)

Velocities m s^{-1}	Ke	Kc	Kec	Ke/Kc	Δke/Δkc
2.5	0.95	1.75E+00	2.7	0.541	0.21
3.5	1.46	3.00E+00	4.46	0.48	0.29
4.5	2.05	4.45E+00	6.5	0.460	0.107

(c)

Velocities m s^{-1}	Ke	Kc	Kec	Ke/Kc	Δke/Δkc
2.5	0.85	1.65E+00	2.5	0.514	0.53
3.5	1.15	2.85E+00	4	0.40	0.187
4.5	1.9	4.30E+00	6.2	0.441	0.3

Tables.6: Volume loss as function of velocities for carbon steel in oil /20% water, at 400mV, and particle size150 –300μm , (a) 15° (b) 45° (c) 90°.

(a)

Velocities m s^{-1}	Ke	Kc	Kec	Ke/Kc	Δke/Δkc
2.5	0.98	1.77E+00	2.75	0.55	0.48
3.5	1.73	3.02E+00	4.75	0.57	0.47
4.5	2.42	4.23E+00	6.65	0.57	0.46

(b)

Velocities m s^{-1}	Ke	Kc	Kec	Ke/Kc	Δke/Δkc
2.5	1.55	1.85E+00	3.4	0.836	0.725
3.5	1.48	3.32E+00	4.8	0.445	0.258
4.5	2.23	4.55E+00	6.78	0.490	0.191

(c)

Velocities m s^{-1}	Ke	Kc	Kec	Ke/Kc	Δke/Δkc
2.5	0.81	1.83E+00	2.65	0.44	0.39
3.5	1.54	2.94E+00	4.51	0.53	0.38
4.5	2.08	4.42E+00	6.5	0.47	0.44

4. Discussion

The effect of impact angles, impact velocities and different particle sizes on the erosion-corrosion of carbon steel in three environments.

In the oil/water environment containing small particle size 150-300μm, the current densities increased with an increase in impact velocity (Figures 3-5(b)). This implies that an increase in velocity increases the corrosion rate of the carbon steel, which is consistent with the findings of Stack et al. [1-3].

This could be due to surface roughening and an increase in exposure area, leading to higher localized dissolution rates on the surface of the specimen. On the other hand, in the crude oil/water environment containing large particle size 600-710μm a similar pattern was observed, with an increase in velocity resulting in a small increase in the overall current densities (Figures 3-5(a)). However, the magnitude of such increases was not as high as in the oil/water environment containing small particle size 150-300μm. The magnitude of the corrosion contribution recorded (kc) (Figures 6-11(a-c)) for carbon steel in the oil/water environment containing particle size 150-300μm and150-300μm indicates that they are not surprisingly in cathodic conditions, i.e. at an applied potentials−400 mV it is at a minimum compared with those recorded at higher applied potential values(0mV and 400mV). However, there is a general increase in total mass loss (kec) with an increase in potential for carbon steel in oil /water environments containing particle size 150-300μm and600-710μm, perhaps indicating that corrosion played the main role in the degradation process [13].The total erosion–corrosion mass losses (Figures 9-11(a-c)) are much lower for carbon steel in oil / water containing particle size 150-300μm compared with t for carbon steel in oil /water containing particle size 600-710μm, which could be due to a decrease in the value of erosion contribution (ke).

Erosion–corrosion maps

The corrosion process can be dissolution, passivation, or transpassivation [1-4]. The erosion–corrosion mechanism map results (Figures 12-14), based on tables 1-6 at three impact velocities, three impact angles with particle sizes 150-300μm and 600-710μm show that at an applied potentials, i.e. -400. The erosion-dissolution regime dominated in oil/ water containing large particle 600-710μm (Figs.12 (a)). The erosion-passivation regime dominated in oil/ water containing small particle 150-300μm and except at intermediate impact velocity 3.5 m s−1 (Figs.12(b)). However, the degree of corrosion appears to be higher for the carbon steel in oil/water containing small particle 150-300μm compared to in environments containing large particle 600-710μm, which is consistent with the mass loss results. The maps indicate, not surprisingly, that the amount of passivation is at a maximum in oil/ water containing small particle 150-300μm (Figures 13-14(b)), where passivation-erosion dominates the majority of the area of the map with an increase in potentials. This could be due to an increase in the passive film due to corrosion product on the surface of the specimen, resulting in passivation–erosion. It is not presence in crude oil/water environment containing large particles sized 600-710μm (Figures 13-14(a)) and erosion –passivation dominates.

However, in the combined environment containing small particles sized 150-300μm (Figures 13-14(b)) the passivation- erosion regime dominates in anodic conditions, which may be due to the impact of particles on the passive film not too great to remove it. Erosion-corrosion additive-synergism maps can be defined depending on whether the erosion-corrosion is additive, synergistic or antagonistic. Additive behaviour is defined as a situation, where the enhancement of corrosion due to erosion (Δkc) [1- 2]. Where corrosion may enhance the erosion ΔKe, this interaction is defined as synergistic behaviour [1, 2 and 3]. On the other hand, where it inhibits erosion, i.e. where the passive film reduces erosion, then the reverse occurs and the mechanism is defined as antagonistic (-ΔKe) ([1- 4]. Both synergistic and antagonistic behaviours are characteristics of erosion-corrosion processes [2, 3]. If the passive film forms on the surface in the exposure conditions and is effective in reducing erosion, i.e. ΔKe/ΔKc> -1, then synergistic should be replaced by antagonistic [1-4].

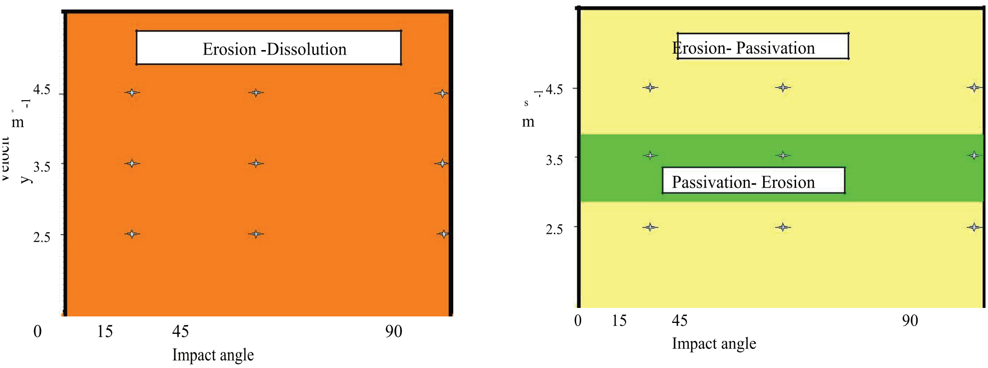

(a) (b)

Fig.12: Erosion-corrosion mechanism maps for carbon steel in oil /20% water environments at - 400 mV (a) 600-710μm (b) 150-300μm

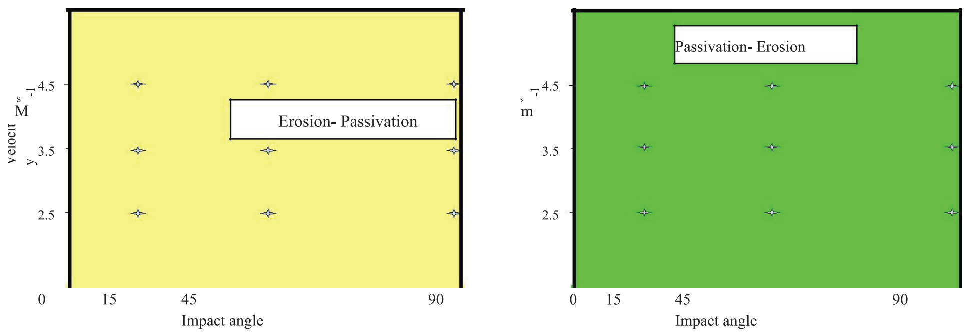

(a) (b)

Fig.13: Erosion-corrosion mechanism maps for carbon steel in oil /20% water environments at 0 mV (a) 600-710μm (b) 150-300μm

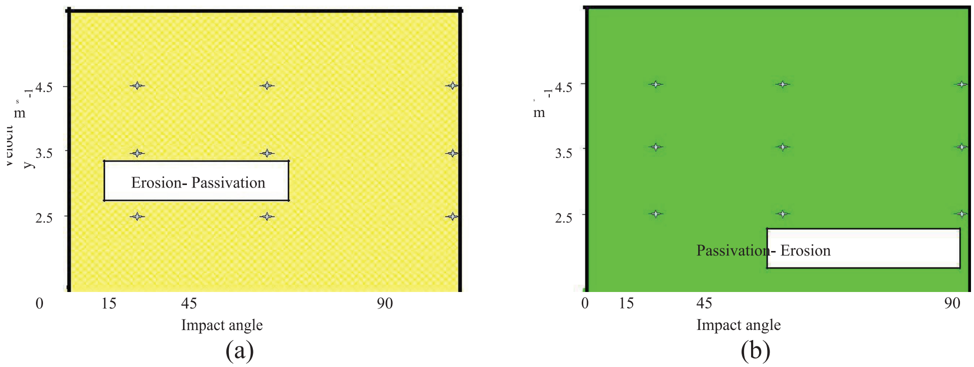

Fig.14: Erosion-corrosion mechanism maps for carbon steel in oil /20% water environments at 400 mV (a) 600-710μm (b) 150-300μm

For the carbon steel in the oil /20%water environments containing large particles sized 600-710μm the synergistic regime dominated where the particles increases wear is observed Fig.15-17(a). On the other hand, the small particles sized 150-300μm the level of synergistic behavior is decreased Fig.15 (b) compared with large particles sized 600-710μm Fig.15-17(a), while the level of additive- synergistic regime occupied the entire maps which indicated to increase the value of corrosion contribution of carbon steel due to changing in the effect of particle size from 600-710μm to 150-300μm. Erosion-corrosion wastage maps (see Figures 18-20 (a-b)) have been constructed based on the results at -400, 0 and 400 mV, where erosion-corrosion regime transitions are presented as a function of velocity and impact angle, and the various contributions are calculated as outlined in tables 1-6. The wastage maps due to erosion-corrosion were constructed according to the following boundary conditions [1-4]:

Kec ≤ 6	Low wastage regime (mg cm $^{-2}$ h^{-1})	4
6 <Kec ≤ 50	Medium wastage regime (mg cm $^{-2}$ h^{-1})	5
Kec> 50	High wastage regime (mg cm $^{-2}$ h^{-1})	6

Figs. 18-20 (a) show erosion-corrosion wastage maps for carbon steel in 20% water with crude oil containing particle sizes 600-710μm. As can be seen, the rate of the medium wastage regime is greater than the low wastage regime, while the low wastage regime dominated with the particle sizes 150-300μm due to the total erosion-corrosion (Kec) having decreased Figs.18-20(b). In addition, there is no evidence of the presence of medium wastage effect on the specimen at low potential of -400mV Fig. 18 (b). Fig.20 (a) shows erosion-corrosion wastage maps for particle sizes 600-710μm at 400mV. The percentage of the medium wastage regime increases with an increase in applied potential. In oil/20% water containing particle sizes 150-300μm at 0 mV and 400mV Fig.19-20 (b), It is interesting to see that the medium wastage regime on the map and it occupied an area at high impact velocity of 4.5 m s^{-1}. The presence of medium wastage regime could be due to an increase in potentials, which indicate an increase in current density and an increase in impact velocity, both of which indicate an increase in the corrosion product removed by the impact particle at high impact velocity. Moreover, it can be seen that the main cause of the medium wastage was the presence of water in the crude oil. The performance maps of the effect of particle sizes have been constructed as function of impact angles and impact velocities at three applied potentials (-400 mV, 0mV and 400mV). Figs.21-23 show the low wastage regime shifted to the intermediate impact velocity of 3.5 m s^{-1}with increase in the applied potential from -400mV to 0 and 400mV and the medium wastage occupied the area at high impact velocity 4.5 m s^{-1} for both a small and large particle sizes Figs22-23.

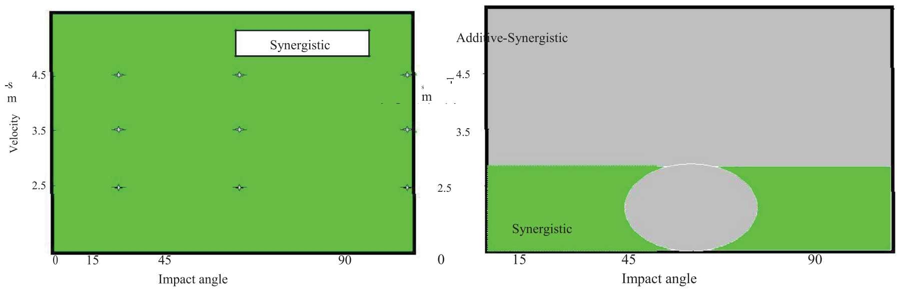

(a) (b)

Fig.15: Erosion-corrosion additive-synergism maps for carbon steel at -400 mV in oil /20% water with particle size (a) 600-710μm (b) 150-300 μm

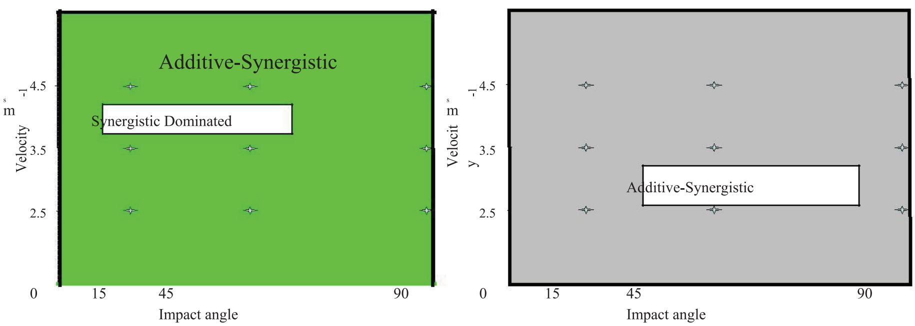

(a) (b)

Fig.16: Erosion-corrosion additive-synergism maps for carbon steel at 0 mV in oil /20% water with particle size (a) 600-710μm (b) 150-300 μm

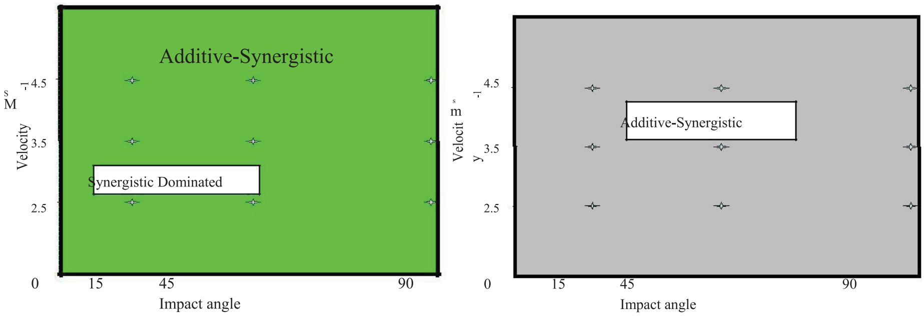

(a) (b)

Fig.17: Erosion-corrosion additive-synergism maps for carbon steel at 400 mV in oil /20% water with particle sizes (a) 600-710μm (b) 150-300 μm

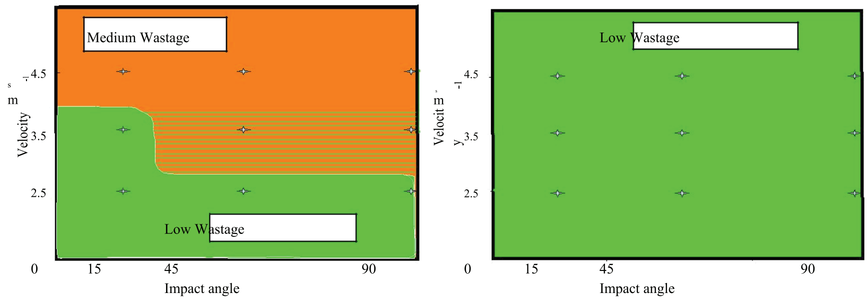

(a) (b)

Fig.18: Erosion-corrosion wastage maps for carbon steel in oil /20% water at -400 mV with particle sizes (a) 600-710μm (b) 150-300 μm

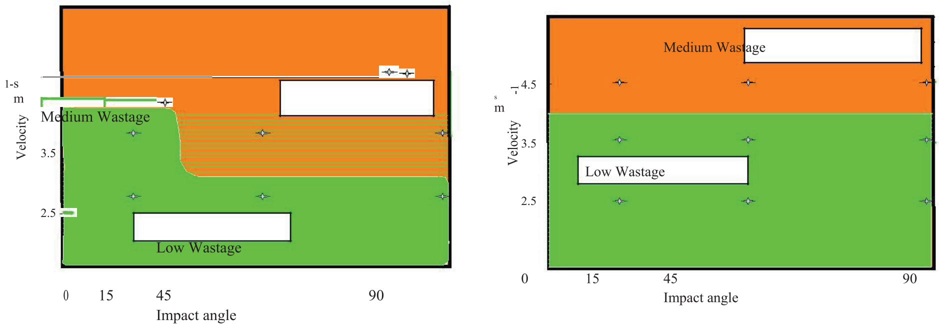

(a) (b)

Fig.19: Erosion-corrosion wastage maps for carbon steel in oil /20% water at 0 mV with particle sizes (a) 600-710μm (b) 150-300 μm

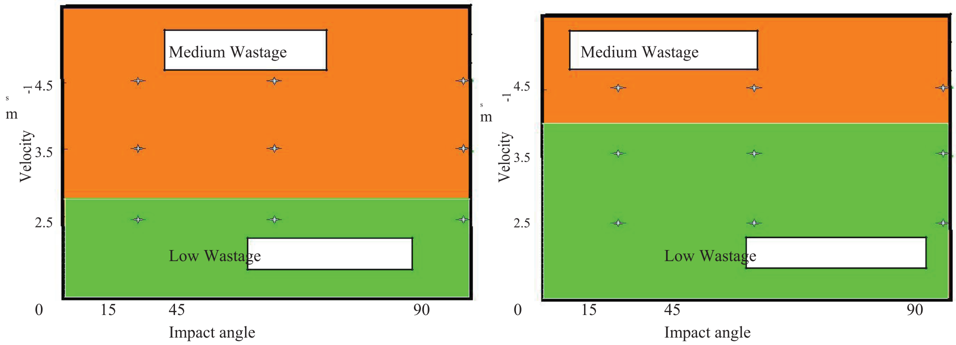

Fig.20: Erosion-corrosion wastage maps for carbon steel in oil /20% water at 400 mV with particle sizes (a) 600-710μm (b) 150-300 μm

Fig.21: Particle sizes performance in oil/20% water environment at -400mV

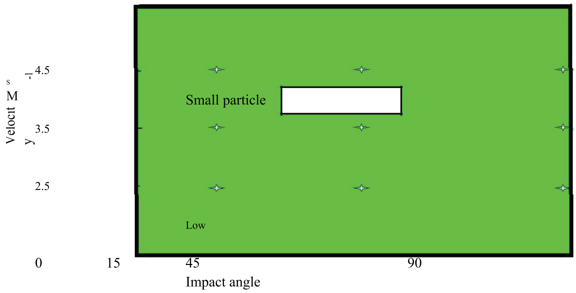

Fig.22: Particle sizes performance in oil/20% water environment at 0 mV

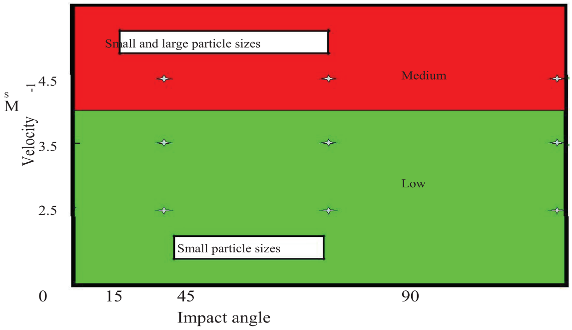

Fig.23: Particle sizes performance in oil/20% water environment at 400mV

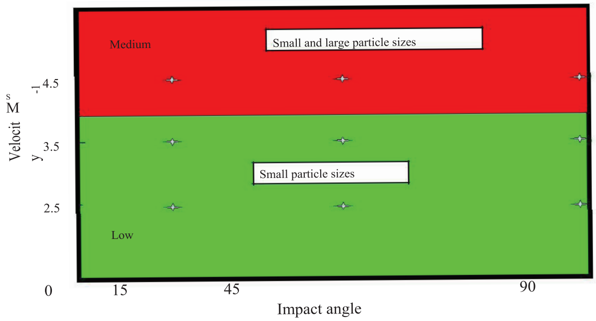

5. Conclusion

The corrosion current density was increased with an increase in applied potential and decrease in particle sized from 600-710μm to 150-300μm.

The effects of impact angles and electrochemical potentials on the erosion–corrosion of carbon steel have been assessed at an impact velocities, potential and impact angle in oil/water environments containing particle sized 600-710μm and 150-300μm. Erosion-corrosion mechanism, wastage and additive-synergism maps have been constructed based on the results. There was no evidence of the presence of a high wastage effect at two particles sized.

6. Reference

[1] M. M. Stack, T. M. Abd El Badia, on the construction of erosion-corrosion maps for wc/co-cr-based coatings in aqueous conditions, Wear 261 (11-12) (2006)1181–1190.

[2] M. Stack, G. Abdulrahman , Mapping erosion-corrosion of carbon steel in oil exploration conditions: Some new approaches to characterizing mechanisms and Synergies, Tribology International, 43 (7) (2010) 1268-1277.

[3] M. M. Stack, S. Zhou and R.C. Newman, Characterization of synergistic effects between erosion and corrosion in an aqueous environment using electrochemical techniques. Corrosion Science, 52 (1996) 934-946.

[4] M.M .Stack and Pungwiwat N, Erosion–corrosion mapping of Fe in aqueous slurries: some views on a new rationale for defining the erosion–corrosion interaction, Wear 256 (5) (2004) 565-576.

[5] R .Hamzah, D.J Stephenson and J.E. Strutt, Erosion of material used in petroleum production, Wear 186 (187) (1995) 493-496.

[6] B. Lawn and R. Wilshaw, Review indentation fracture: principles and applications, Journal of Material science, 10 (1975) 1049-1081.

[7] M.V. Swain and J.T Hagan, Indentation plasticity and the ensuing fracture of glass, Journal of Physics (1976) 9 2201.

[8] M. M. Stack, Y. Purandare, P. Hovsepian, Impact angle effects on the erosion-corrosion of superlattice crn/nbn pvd coatings, Surface & Coatings Technology 188(2004)556–565.

[9] J.B. Zu, I.M. Hutchings and G.T. Burstein, Design of a slurry erosion test rig, Wear140 (2) (1990)331–344.

[10] M.M. Stack, T. M. Abd El Badia, Mapping erosion–corrosion of WC/Co–Cr based composite coatings: particle velocity and applied potential Effects, Surface& Coatings Technology 201(3-4) (2006)1335–1347.

[11] G.T .Burstein, Y. Li and I.M. Hutchings, The influence of corrosion on the erosion of aluminum by aqueous silica slurries, Wear 186-187 (Part 2) (1995) 515 – 522.

[12] X .Tang, L.Y. Xu and Y.F. Cheng, Electrochemical corrosion behavior of X-65 steel in the simulated oil–sand slurry. II: Synergism of erosion and corrosion, Corrosion Science, 50 (2008) 1469–1474.

[13] S.S. Rajah Ram, T.J. Harvey, R. J. K. Wood, Erosion–corrosion resistance of engineering materials in various test conditions, Wear 267 (2009) 244–254